2004 Undergraduate Thesis, Barnard Physics Department

The Search for Radio Stars at the Nano-Jansky Scale

Regina M. Flores

Barnard College Physics,3009 Broadway,NY,NY,10027

David J. Helfand and Eilat Glikman

Columbia University Astrophysics,550 West 120th St.,NY,NY,10027

ABSTRACT

Using known optical stellar positions observed by the Hipparcos Satellite we searched for stars with radio emission using the FIRST survey. A stacking technique developed by Glickman et al. was employed in order to detect radio stars at the nano-Jansky scale. No detections were found, but a limit can be determined of the minumim background necessary for detecting radio stars by evaluating the root-mean-square of the image background.

1. INTRODUCTION

1.1. *A Brief History of Radio Stars*

[1] In studying the history of radio astronomy, one finds that its contribution to our understanding of the universe has been monumental. Although a relatively recent observational technique, radio astronomy has been a pivital tool in probing corners of our Galaxy and beyond never before imagined. In fact, one might go so far as to say that one of the most influential and revolutionary discovereries of the 20th century was Karl Jansky's 1933 detection of radio emission from the Sagittarius constellation. It was this serendipitous experiment that gave way to the birth of radio astronomy and spawned an interest in further discoveries from the "mysterious" radio waves propagating from space into Earth's sky. In 1937, a young and determined scientist by the name of Grote Reber built a telescope 31.4 ft in diameter in his own backyard after being denied employment with Bell Laboratories (the institution

[1]Information courtesy of http://www.nrao.edu/whatisra/history.shtml

responsible for the Jansky experiments). His nightly sky scanning produced, in 1938, clear confirmation of the Janksky discovery of radio emission from the Milky Way. Among other discoveries, Reber was the first to note the inverse power law for radio frequencies; i.e., power decreases at higher frequencies. Figure 1 shows a graph of this relationship.

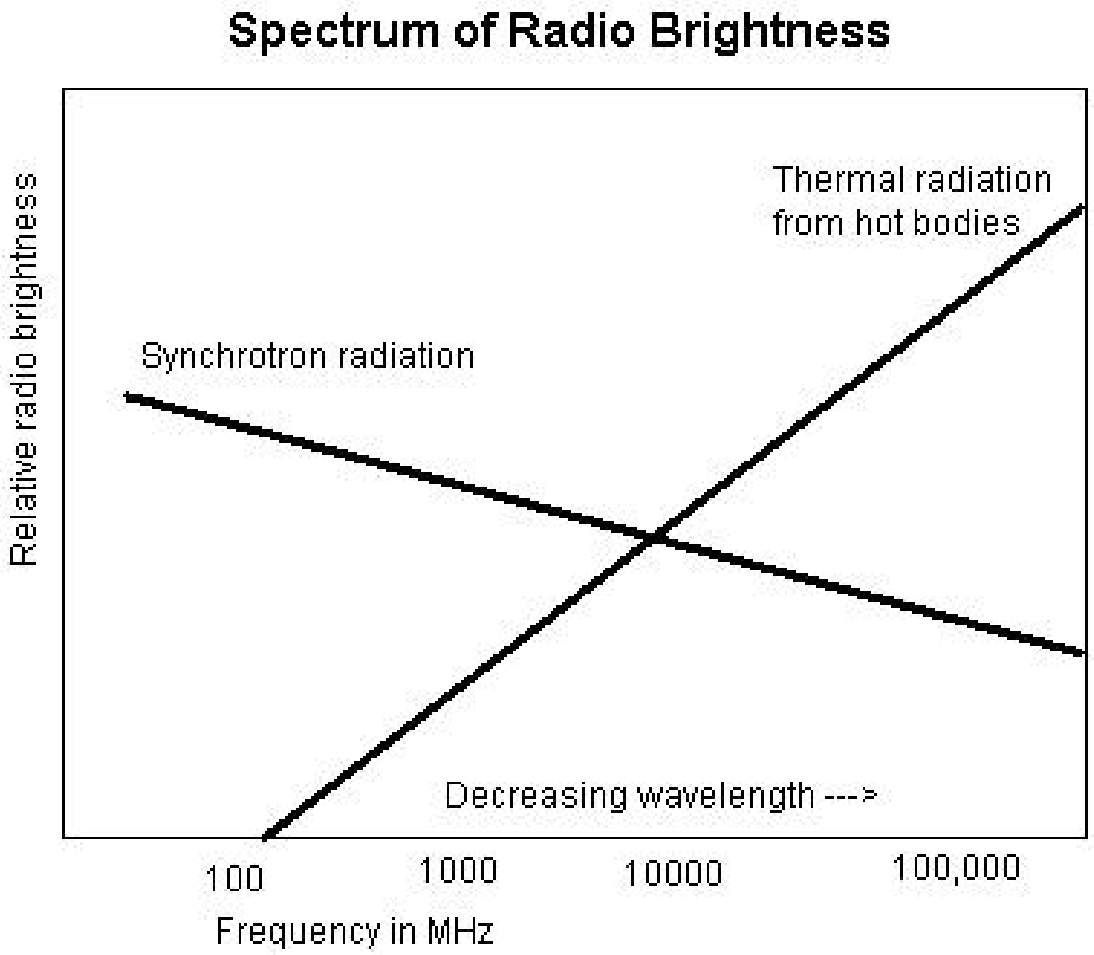

Fig. 1.— The spectrum of radio sky brightness.(Image courtesy of http://www.nrao.edu/whatisra/hist_reber.shtml)

Although Reber was among the first scientists to discover radio sources in our Galaxy, such as Cygnus and Cassiopeia, it was not until 1942 that J.S.Hey detected radio emission from the Sun. This proved to be the first discovery of radio emission from a *star* and introduced new questions into the minds of astronomers, namely: if the sun is a star and it emits radio waves, then are there more radio emitting stars in and outside of the Milky Way galaxy? The answer to that pertinent question, although intriguing to many scientists at the

time, lay virtually unanswered for the next few decades due to the lack of available resources such as large, powerful telescopes that are required to search for radio stars. However, the second half of the 20th century marked a pivotal turning point in radio star detection thanks to the opening of the National Radio Astronomy Observatory (NRAO) Green Bank interferometer, in 1970, and, most importantly, the NRAO Very Large Array (VLA), in 1980. The two observatories were perhaps two of the world's premier radio observing centers and have both contributed immensely to the advancement of our understanding of radio stars vis-a-vis the numerous sky surveys that have been conducted using these instruments. However, after almost 20 years of studying the radio properties of stars there have been relatively few detections. Could it be that we are just not probing deep enough or that our instruments are not sensitive enough to detect radio emission from stars?

Today with our ever-expanding wealth of sky surveys from different regions of the electromagnetic spectrum and increased computing power, it is possible to search for radio stars on scales never before imagined. We hope to show in this paper that by employing new computing methodologies and technologies, finding radio stars, down to the nano-Jansky scale, is not only possible but the beginning of a new wave of radio astronomy.

2. THEORY OF RADIO STARS

2.1. *What are Radio Stars?*

In order to search for radio emitting stars one must first ask a fundamental question: What is the definition of a radio star? A radio star is defined[2], for a brightness temperature, T_B, and an average solid angle over a region where the source is emitting, Ω_s, such that its flux density is given by,

$$S_\nu = \frac{2k\nu^2}{c^2} T_B \Omega_S \tag{1}$$

Defining a disk diameter, $\Omega_s = \pi\theta^2$, we can rewrite the equation as follows:

$$S_\nu = \frac{T_B \theta^2}{1970\lambda^2} \tag{2}$$

We know a radio telescope can detect a radio star if the following expression is met:

$$T_B \theta^2 \geq 1970\lambda^2 S_{min} \tag{3}$$

[2]Hjellming,p.383

where S_{min} is the minimum flux density measured. So we see that what ultimately governs a radio star's detectability are its brightness temperature and the angular diameter of its emitting region. However, since the angular diameter of a radio star is almost always very small, the surface brightness parameter is going to dominate. So does that mean we can only detect radio stars that have high flux density levels? Not necessarily! Stars with unusually large angular sizes have been observed in the past few decades. Thus to detect radio stars any combination of high surface brightness temperatures or large size scales will constitute a good candidacy for radio stellar detections. Figure 2 shows a plot of the main sequence, demonstrating radio star detection as a function of stellar magnitudes and spectral type.

2.2. *Radiation Processes: Why does a Star Emit Radio Waves?*

A more fundamental question seems relevant in understanding and searching for radio stars: Why do stars emit radio waves? The answer to that question lies in the radiation process known as the thermal bremsstrahlung radiation or free-free radiation. Bremsstrahlung radiation is the radiation due to accelerating charges in the electromagnetic field of another charge[3]. This occurs when there are two different particles[4] like an electron and an ion in an ionized plasma. The Gaunt factor, a function of the energy of the electron and the frequency of the emission, is used to quantify the ratio of the exact to the semiclassical value of emissivity as the electrons are scattered by the ions. It is defined as

$$g_{ff}(\nu, w) = \frac{\sqrt{3}}{\pi} ln(\frac{b_{max}}{b_{min}}) \tag{4}$$

Specifically for validity at radio waves, the Gaunt factor approximation is

$$g_{ff}(\nu, T_e) \cong 1.38 {T_e}^{0.16} {\nu_{GHz}}^{-0.1} \tag{5}$$

where T_e is the electron temperature. The emission coefficient for free-free emission is

$$j_v \rho \cong 7.45x10^{-39} {N_e}^2 {T_e}^{-0.34} {\nu_{GHz}}^{-0.11} \tag{6}$$

where N_e is the electron concentration. Thus these two expressions can be related by the Plank function for blackbody radiation by

$$\frac{j_v}{\kappa_\nu} \cong 2kT_e(\frac{\nu}{c})^2 \tag{7}$$

where k is Plank's constant.

---

[3]Rybicki

[4]Since the bremsstrahlung radiation due to a collision of like particles, such as an electron with another electron, is zero in the "dipole approximation".

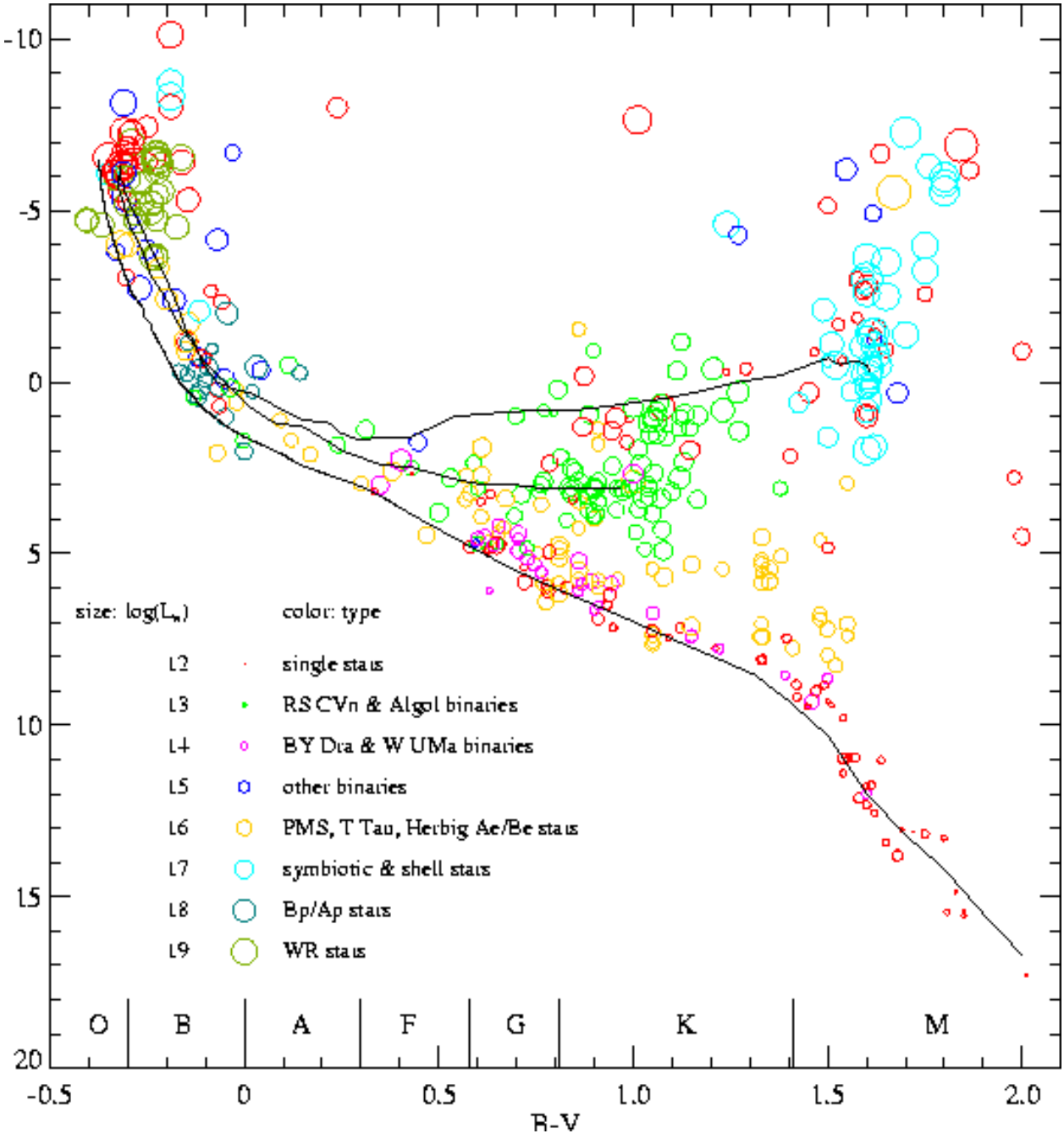

Fig. 2.— Image of the HR diagram with radio star sources superimposed.(http://www.ras.ucalgary.ca/SKA/science/node13.html)

3. THE FIRST SURVEY

In 1993 the world's first unbiased survey known as the Faint Images of the Radio Sky at Twenty-cm (FIRST) Survey began at the VLA in Socorro, New Mexico (see figure 3). The

Fig. 3.— Image of the VLA. (Image courtesy of http://www.nrao.edu/imagegallery/php/level3.php?id=90)

survey was taken using the VLA in the B-configuration with fourteen 3 MHz channels centered at 1400MHz. Overlapping "snapshots" of 165s were taken along a constant declination to obtain a grid of images. FIRST covered over 8,500 square degrees of the North Galactic Cap and a smaller section of the South Galactic Cap see figure 4. There are about 811,000 sources detected in FIRST with a positional accuracy down to 1mJy of better than 1".

4. THE HIPPARCOS AND TYCHO MISSION SURVEY

The Hipparcos Space Astrometry Mission telescope (see figure 5) was launched in 1989 and produced the world's most accurate measurements of position, parallax and proper motions of stars. In addition, the Hipparcos mission is unique in that one of its main scientific

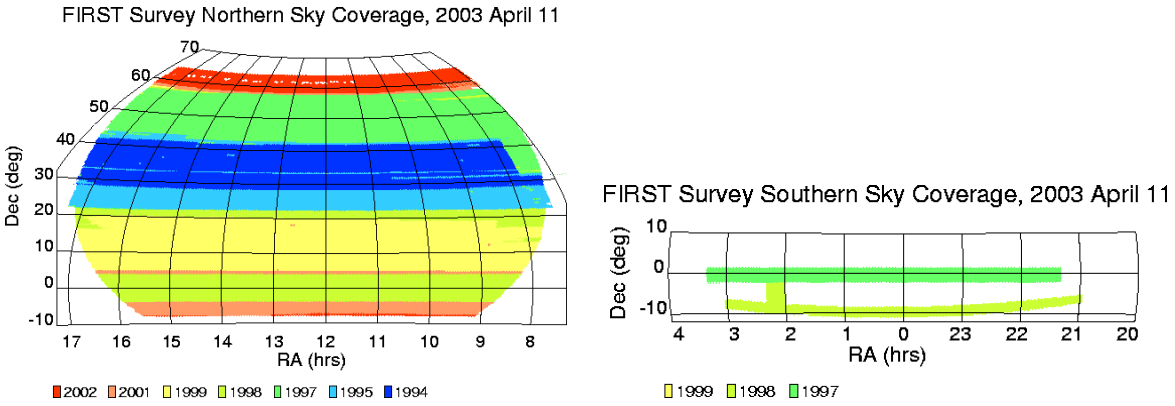

Fig. 4.— Left: North coverage area. Right: South coverage area.(Images courtesy of http://sundog.stsci.edu/first/obsstatus.html)

objectives is to provide a point of reference, vis-a-vis a "non-rotating stellar reference frame" within our Galaxy, for correlation to observations made in other regions of the electromagnetic spectrum. In other words, the Hipparcos Mission serves to link the EM spectrum for multi-wavelength astronomy. During its seven-year lifetime, the Hipparcos experiment located approximately 120,000 stars with 1 milliarcsec-level astrometry and approximately one million stars with 20-30 milliarcsec astrometry and two-color photometry, the latter data referring to the Tycho experiment. The catalogs and all subsequent technical information can be found on the Hipparcos Mission website[5].

5. THE EXPERIMENT

The goal of our experiment is to discover local radio stars using known optical positions from the Hipparcos and Tycho Surveys and to correlate them to the positions within the FIRST survey. This is done by using stacking techniques developed by D.J Helfand, E. Glikman and their collaborators. The technique used to search for radio stars employs a statistical algorithm that, by averaging many FIRST images centered on known optical stellar positions, we can detect the mean flux density of a population of objects to far below

[5]http://astro.estec.esa.nl/Hipparcos/

the FIRST rms noise down to flux densities on the order of hundreds of nano-Janskys[6].

6. THE STACKING METHOD

6.1. *The Program*

At the heart of this entire project is the statistical algorithm that averages, or stacks, radio images to produce mean flux densities for sources that are individually below the noise of the original image. Thus a brief description of the inner workings of this algorithm is necessary. Using the IDL programming language, a program was designed, originally by E.Glickman and later modified by S.Hu and R. Flores, to do the following tasks:
1) Reads in the 33 x 33 pixel images into a 3 dimensional array of 33 pixels x 33 pixels x number of total images. This is done by using the READFITS function from the FITS/IO section of the IDL Astronomy functions. It calls an array of strings that correspond to the directory path name where the images are stored on disk.

2) Calculates the background noise of each image. This is done by calling upon an external IDL program designed by E. Glikman with modifications made by R.Flores. The program breaks a square image into four strips (top, bottom, left and right) and a 5x5 pixel box at the center. It then discards the central box by cutting out the strips and turning them into one dimensional arrays in order to perform various statistical tests who's values are returned to the stacking program.

3) Calculates the maximum pixel value of each image. This is done by an internal IDL function called MAX which returns the maximum value in an array.

4) Filters out subsets of the stellar population using specific criteria specified by the user. As will be described in detail later, different selection criteria for different stars were made. They were then filtered out using the IDL's WHERE function that simply identifies the addresses of the elements in an array which meet the criteria and stores them into a new array.

5) Filters out sources brighter than 0.5mJy. Since we are looking for "faint"stars–i.e, stars that have never been detected in the radio before– we arbitrarily concluded that a 0.5mJy cutoff was a conservative choice. The WHERE command was also used here.

---

[6]It is important to note that this technique is not unique to stars and can be applied to other radio sources, for example quasars (see Glikman et al. 2004).

6) Filters out images in which there is a bright radio source in the region of sky near the star. Selecting the maximum threshold number for the peak pixel value of the background region in any given image, given by:

$$\max_{bkgd} \leq 1.5 \times \frac{(0.15 \times 10^{-3})}{\sqrt{N}} \times N$$

where 1.5 σ is the maximum contribution any source is allowed to make to the stacked image, 0.15×10^{-3} is the average root-mean-square noise level for images in the FIRST survey and N is the number of images in a sample. We know that the rejection criteria for the background should change depending on how many images we include in the sample. So the next question is, how do we determine the criteria? Each image has both a standard deviation for the background and the source pixels and therefore each image has its own statistics. When you average all the images in a sample, you are left with one final image with its own final statistics. So when you choose a threshold value for a given list of images or sample, you do not want to choose a threshold that is too high such that it deviates from the total average. The average standard deviation of one image is given by:

$$\sigma_{\overline{x}} = \frac{\sigma_x}{\sqrt{N}}$$

For the FIRST survey, the mean measured $\sigma_x = (0.15 \times 10^{-3})$.[7] Therefore,

$$\sigma_{\overline{x}} = \frac{(0.15 \times 10^{-3})}{\sqrt{N}}$$

and,

$$\frac{Signal}{Noise} = \frac{Maxpixel}{\sigma_{\overline{x}}}$$

Based on the properties of the Poisson distribution and the fact that in our case the flux from the signal is the maximum pixel from the source and the standard deviation is the noise of the surrounding image, then it follows that

$$\frac{Maxpixel}{N} \leq 1.5\sigma_{\overline{x}}$$

and we see that

$$\frac{Maxpixel}{N} \leq 1.5 \times \frac{(0.15 \times 10^{-3})}{\sqrt{N}}$$

and therefore

$$\max_{bkgd} \leq 1.5 \times \frac{(0.15 \times 10^{-3})}{\sqrt{N}} \times N$$

[7]Becker et al.

To obtain this filter the WHERE function was used with a limitation called FINITE which constrains the output to only elements in the array which are non-infinite.

7) Stacks the images by summing all remaining images and dividing by the total number of images used. This was done using the TOTAL function.

8) Creates a final image in the .fits format. This was done by using the IDL WRITEFITS function as well as SXADDPAR function to add information to the header file of the images.

6.2. *Calibration*

In the early phases of this project, a series of in-depth analyses and tests were made in order to verify the validity of the stacking algorithm, identify (if any) a CLEAN bias, and verify the robustness of the FIRST pipeline (the data reduction script, or the "chain of commands", if you will, that the data passes through in order to produce a final processed image). To do this, "fake" or artificial data was made using the AIPS UVMOD routine by R. Becker (see Becker et al.). Artificial point sources were placed 40″ away from each other on a 10' x 10' grid as shown in figure 6. A program was written in the IDL programming language by E. Glikman to identify sources in an image, cut out a box around the source, then stack up all the boxes to obtain a final image. The key element in this routine is the position parameter used to account for the Cartesian nature of the data. However, since the artificial data was not uniformly placed in the same grid pattern, an additional program was written by R. Flores. This program, instead of using an internally defined source position, was designed to use an external definition of the source position called from the header file of the image known as the GPOS parameter. Both programs were run for 5 different tests: 1) "No Clean"- data that had not been passed throughout the clean process in order to check for a clean bias, 2) "No Pipe"- data that had not been passed through the FIRST pipeline in order to check for pipeline "breakdowns", 3) "200μJy"- data using 200μJy sources, 4) "80μJy"- data using 80μJy sources, 5) "40μJy"-data using 40μJy sources. The AIPS data reduction software was used for analysis on each of the 10 images resulting from the tests, as per table 1. We see that the GPOS correction routine produces the same results as the position-defined routine, thus proving that the position definitions are in fact correctly implemented and the GPOS is in fact not necessary. We also found that the peak pixel values and the initial input values do not agree. In fact, the input values are all about 60% greater than the measured values. Figure 7 shows the linear relationship of the input and measured values with a linear fit of exactly 0.6 units.

Although we are certain of the 60% calibration bias, we are not certain where the bias

Table 1. Calibration Results

Map name	Input Val. (Jy)	Peak (Jy/beam)	Baseline (Jy)	X pos. (pixels)	Y pos. (pixels)	Fitted Major	Fitted Minor	Num Images	Num Used	Num Reject
noclean	4.E-05	-2.1E-05	-9.9E-06	8.481	3.247	9.407	1.766	55400	55328	72
nocln-gpos	4.E-05	-2.1E-05	-9.9E-06	8.481	3.247	1.766	1.766	55400	55328	72
nopipe	4.E-05	2.5E-05	-1.4E-07	6.014	6.001	3.211	2.382	55400	55395	5
nopipe-gpos	4.E-05	2.5E-05	-1.4E-07	6.014	6.001	3.211	2.382	55400	55395	5
test200	2.E-04	1.2E-04	-3.3E-06	5.994	6.001	3.239	2.374	67100	67098	2
test200-gpos	2.E-04	1.2E-04	-3.3E-06	5.994	6.001	3.239	2.374	67100	67097	3
test80	8.E-05	5.1E-05	-9.8E-07	6.006	5.967	3.238	2.372	67100	67095	5
test80-gpos	8.E-05	5.1E-05	-9.8E-07	6.006	5.967	3.238	2.372	67100	67095	5
test40	4.E-05	2.7E-05	4.8E-08	6.003	6.011	3.146	2.383	45300	45295	5
test40-gpos	4.E-05	2.7E-05	4.8E-08	6.003	6.011	3.146	2.383	45300	45295	5

is coming from. One hypothesis is that the grid pattern of the artificial data is introducing its own bias. Current tests are underway to remove the grid and introduce randomly placed sources. The results will be interesting in our understanding of the intrinsic nature of the data, but do not effect the results of this paper. The 60% bias is simply taken into account in our final analysis.

6.3. *Star Stacking Procedure*

The Hipparcos and Tycho catalogs were obtained from the online Hippparcos Survey database. A table that contained the right ascension and declination, the "name", of each star as well as numerous other data was downloaded. There are a total of 118,218 stars in the Hipparcos catalog and a total of 1,058,332 stars in the Tycho catalog. The table, containing about 100 columns, was shortened by selecting only those columns that are pertinent to our experiment[8]. The documentation specifying the table's perameters was found on the Hipparcos Mission website under section 2.1 and 2.2 of Introduction and Guide to the Data: Volume 1.

We discarded all the stars that fell outside the FIRST survey coverage area (see Figure 4). Next we used a program designed by R. White in the Python programming language to, for each stellar position, extract a 1 arcmin FIRST image, called a "cutout", centered on the star's RA and DEC and then store the image to disk. A total of 22,792 cutouts for Hipparcos and 129,008 cutouts for Tycho were used. The entire Hipparcos and Tycho cutout images were stacked using the stacking program. Because, however, the Tycho catalog is on the order of 100 thousand stars and IDL cannot store in memory such a large quantity of data at one time, processing the Tycho catalog in its entirety proved to be impossible. The Tycho catalog was thus broken up into four data files, each file containing 32,252 stars, and each piece was stacked. Then the four resulting images were combined in IRAF using the IMCOMBINE function. From figure 8 we see that there were no detections made by stacking the entirety of either catalog. We therefore decided to make stacked images based on stellar magnitudes and spectral types.

Histogram plots were made in order to determine how to constrain the data (refer to Figures 9 through 14). The plots were generated using the PLOTHIST function in IDL. Figure 9 shows the histogram for color index. We divided the bins by spectral type for M,

[8]Although this step seems trivial, in reality it proved to be one of the most lengthy processes due to the number of lines in each document. In order to format the text documents for the specified formats of the programs a VI shell script was used in addition to a combination of unix command line file manipulations.

K, G, and F stars. Since our goal was to locate nearby stars, and Giant stars are much farther away, it was determined that we would use the Dwarf stars. Referring to a Stellar Data table[9] of main sequence stars, we were able to calculate a range of color index for each spectral type. We were also able to determine a distance criteria based on the absolute luminosity as compared to the magnitude limits of the respective catalog. Tables 2 and 3 outline the selection criteria. Note that all images were made for stars with a proper motion less than 200mas yr^{-1}.

The stacking program, outlined in section 6.1, was run for each of the selections. In order to optimize the stacking program both the catalogs were filtered through a program designed by E. Glikman called CLEAN-UP. This program is designed to select only the data that the selection criteria calls for, thus eliminating extraneous data and saving space in memory. Figures 15 through 22 show each of the stacked images for the Hipparcos selection criteria. Figure 23 shows the stacked images for the Tycho selection criteria. There were no detections found in either catalog for any selection criteria.

6.4. *Excluded Sources*

An additional analysis was made of the rejected sources from the Hipparcos catalog by the filter that excluded sources brighter than 0.5 mJy. There were 447 excluded sources found. The RA and DEC of each source was input into the Extract Cutout program found on the FIRST website. For each source position a 1x1 arcmin image, scaled to 1mJy, was produced. Using the "eye-balling" technique, each image was analysed to see if a star-like source was present. Figure 24 is what a typical source detection would look like. All the images that were either noise, some other source with extended radio emmission or a source too faint to distinguish from the noise were discarded from the list. These sources were compared to the Helfand, Schnee et al. paper where 26 radio stars were detected. The sources on our list that corresponded to sources in Helfand, Schnee were also discarded. There were a total of 41 remaining sources. Theses remaining sources were then input into the FIRST Catalog Search program on their website to obtain data about each source. In addition, the sources were inputed into the HEASARC database to compare to known X-ray sources. This was done because there is a strong correlation between X-ray and radio emission from stars. A similar analysis was made for the Tycho catalog. There were a total of 2474 excluded sources found in Tycho. These sources have not yet been analysed. Due to time constraints, the results are not published in this paper. For further questions of the

[9]Appendix E, Carrol and Ostlie

Table 2. Selection Criteria for Hipparcos Catalog

Spectral Type	B-V less than	B-V greater than	Distance Less than (pc)	Distance greater than (pc)
Nearby M Stars	-	1.4	20	20
K-Dwarfs	1.4	0.8	100	100
G-Dwarfs	0.8	0.58	200	200
F-Dwarfs	0.58	0.3	450	450
F-Dwarfs	0.3	-	-	-
All	-	-	25	10
All-Hist. Status	-	-	50	-

Table 3. Selection Criteria for Tycho Catalog

Spectral Type	B-V less than	B-V greater than	Distance Less than (pc)	Distance greater than (pc)
Nearby M Stars	-	1.4	-	-
K-Dwarfs	0.8	0.58	-	-

X-ray correlation contact the author.

7. RESULTS

Although neither catalog produced a detection of stars, we do have some interesting results. First, we can conclude from these analysis that no detections will be made above the background of the stacked images. So, for instance, if an astronomer wanted to observe the sky with a radio telescope and search for stars she would have to calculate the exposure time to at least detect the background level of our images.

The Tycho catalog also produced some interesting results. In the stacked image from Tycho there are "holes" at the center of the image or the center pixels have negative flux densities, the opposite of what we hoped to find. Although this discrepency has yet to be understood, one theory as to why these negative "valleys", as opposed to positive peaks, are appearing is due to the two different filters we use for the center 5X5 pixels and for the background. One of the major issues in radio astronomy is the "clean" process. Every radio source has what are called side lobes. The clean process removes the side lobes, but the FIRST survey only cleans those sources that are greater than 1.0mJy. Of course in the center we reject those sources as well. So what about the sources in the background that are brighter than 1.0mJy? It was suggested that because our central 5x5 filter was so strict, i.e no pixel is allowed above 0.5mJy, we were inadvertantly allowing negative side lobes, from sources in the background, to enter. Thus it could be that we were in fact detecting radio sources but since they are faint the negative side lobes were dominating and thus yielding the "holes". Shifting the source positions in the Hipparcos and Tycho catalogs by an arbitrary amount and stacking them would yield background images, which could later be subtracted from the stacked source images in order to yield a correction to the data.

8. CONCLUSION

In the scope of an undergraduate research thesis there is not enough time and resources to complete this project. Devising tests to determine a correction to the background of the Hipparcos and Tycho catalogs would not only produce results pertinent to the search for radio stars, but it would also help scientists to both understand the nature of radio data and the possibilities of nano-astronomy. Further investigation would also overlap into other studies of radio sources, like quasars for example, as well as have interesting implications of sources that exist in both the radio as well as in other regions of the electomagnetic spectrum.

I wish to thank the faculty and staff of the Columbia Astrophysics Departments for their support of my education and training in pursuit of my degree. In particular I would like to thank D.J Helfand for giving me the opportunity of a life time and believing in my potential as a scientist. I would like to give a very special thank you to E. Glikman who opened the doors for me and who continues to inspire me, with her unyielding enthusiasm, to follow my dreams. I would also like to thank the Barnard Physics Department, in particular L. Kay and T. Halpin-Healy, for their academic advising and monitoring and for their continued devotion to the education of aspiring women scientists. I would also like to acknowledge Barnard College for their financial support of my education in order to "change the world one woman at a time."

REFERENCES

Becker, R. H., White, R. L., & Helfand, D. J., ApJ, 450, 559

[] Carrol, B. W.& Ostile, D. A., An Introduction to Modern Astrophysics, (New York: Addison-Welsley Publishing)

Glikman, E., Helfand, D. J., Becker, R. H., & White, R. L. 2004, in ASP Conf. Ser. VOLUME, AGN Physics with the SDSS, ed. G. T. Richards, & P. B. Hall, PAGE

Helfand, D. J., Schnee, S., Becker, R. H.,White, R. L., & McMahon, R. G. 1998, ApJ, 117, 1568

Hjellming, R. M., in Galactic and Extragalactic Radio Astronomy, ed. G. L. Verschuur et al. (New York: Springer-Verlag), 381

Rybicki, G. B. & Lightman, A. P., Radiative Processes in Astrophysics, (New York: A Wiley-Interscience Publication, 1979)

Fig. 5.— Image of the Hipparcos and Tycho telescope. (Image courtesy of http://www.esa.int/esaSC/120366_index_1_m.html)

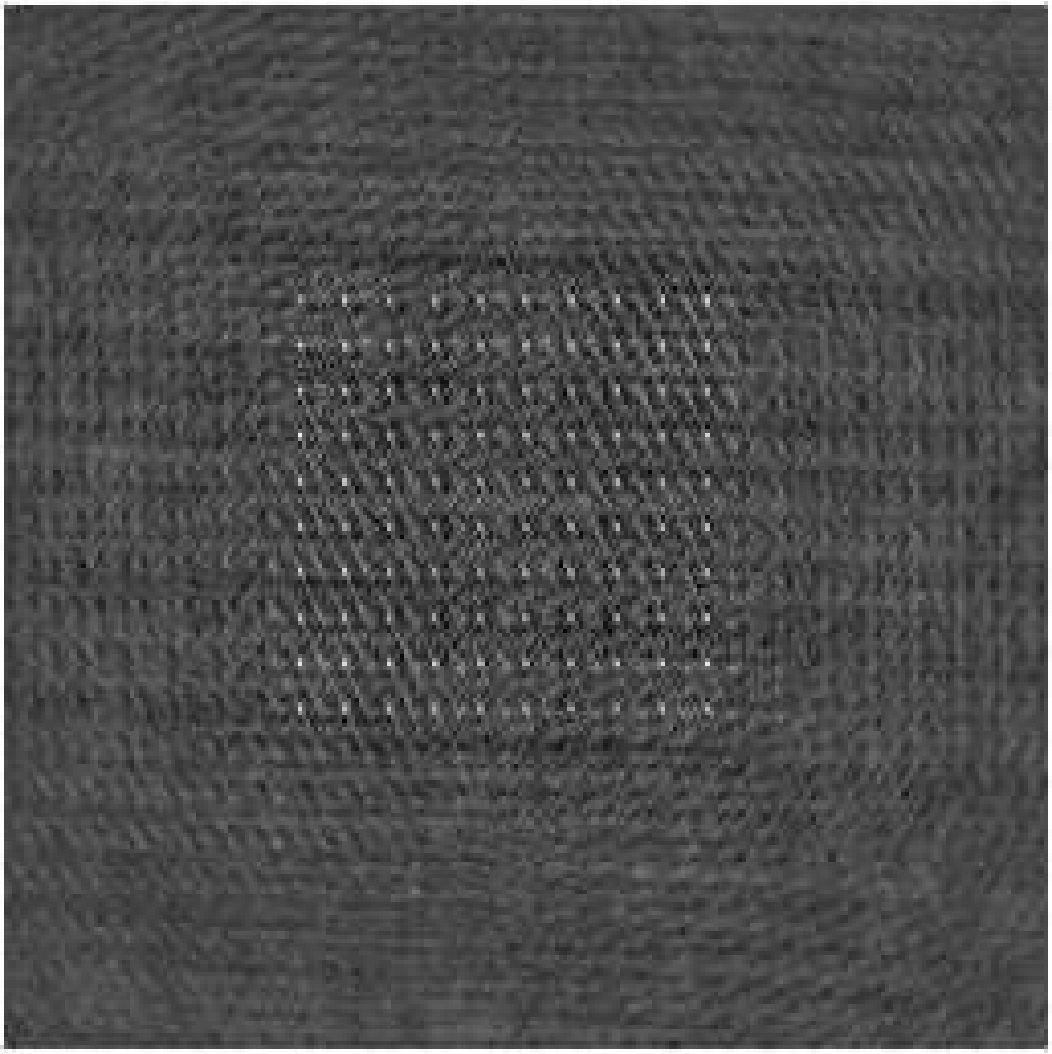

Fig. 6.— Image of the grid pattern of the artificial data.

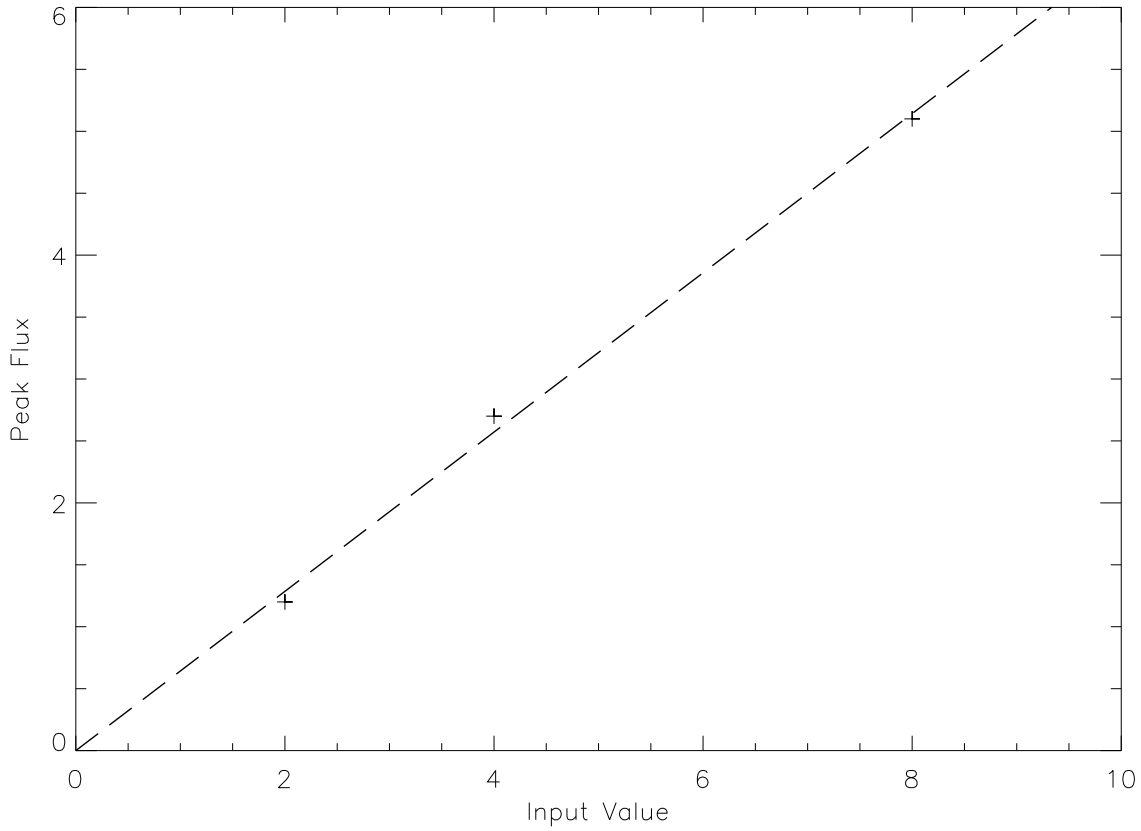

Fig. 7.— Linear fit to the data showing 60% bias.

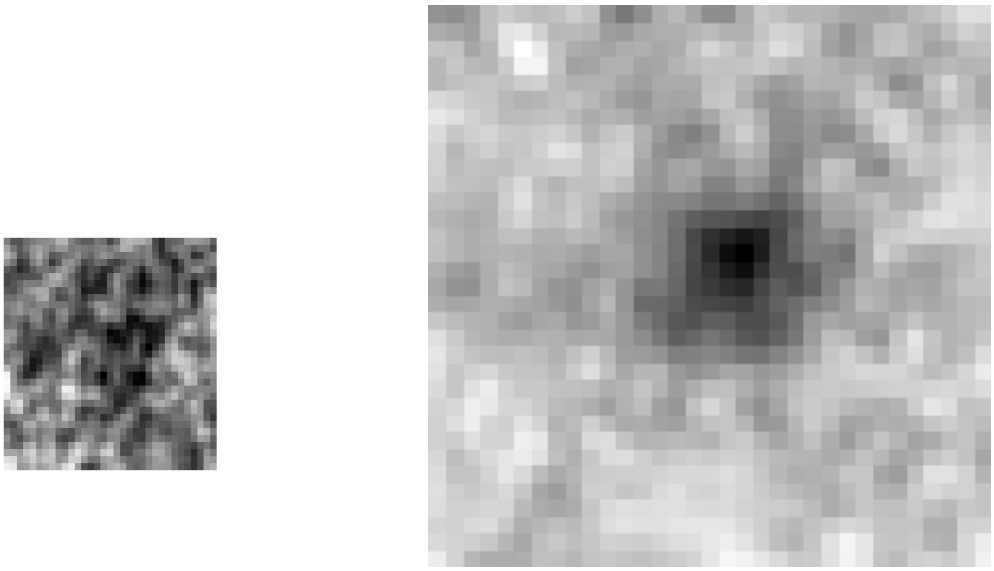

Fig. 8.— Left: Image of all stacked Hipparcos images. Image RMS 2.53E-02.Total number of stacked images is 22,323. Right: Image of all stacked Tycho images. Image RMS is 4.48E-07. Total number of stacked images is 126,447.

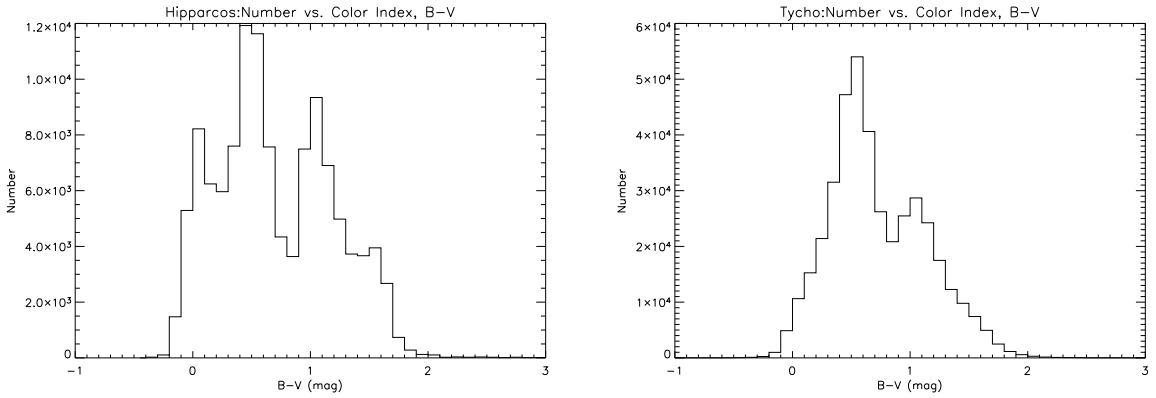

Fig. 9.— Histogram to determine spectral type selections.Left:Hipparcos. Right:Tycho.

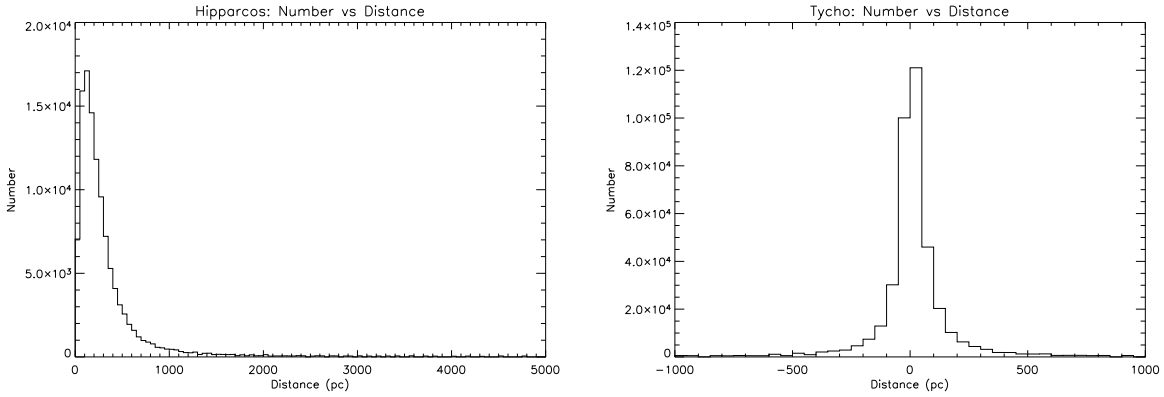

Fig. 10.— Histogram to determine distance criteriaLeft: Hipparcos. Right: Tycho.

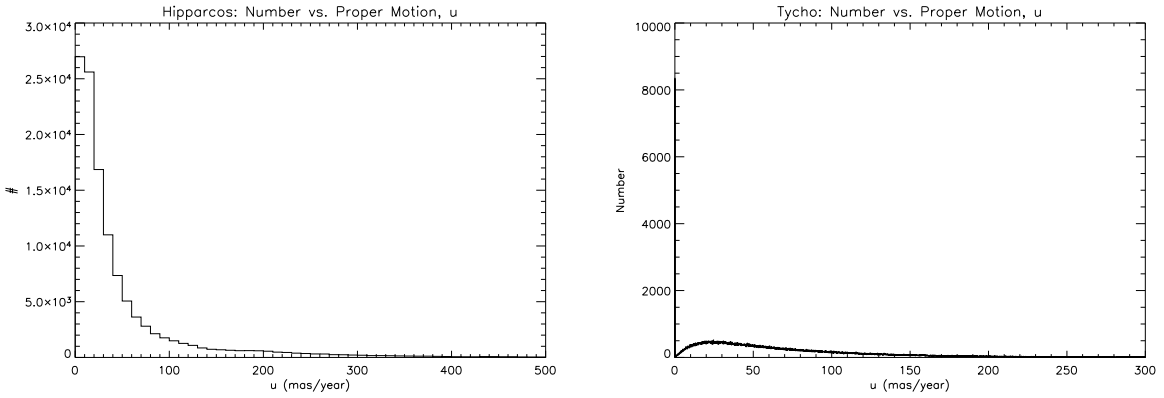

Fig. 11.— Histogram to determine proper mottion criteria. Left:Hipparcos.Right:Tycho.

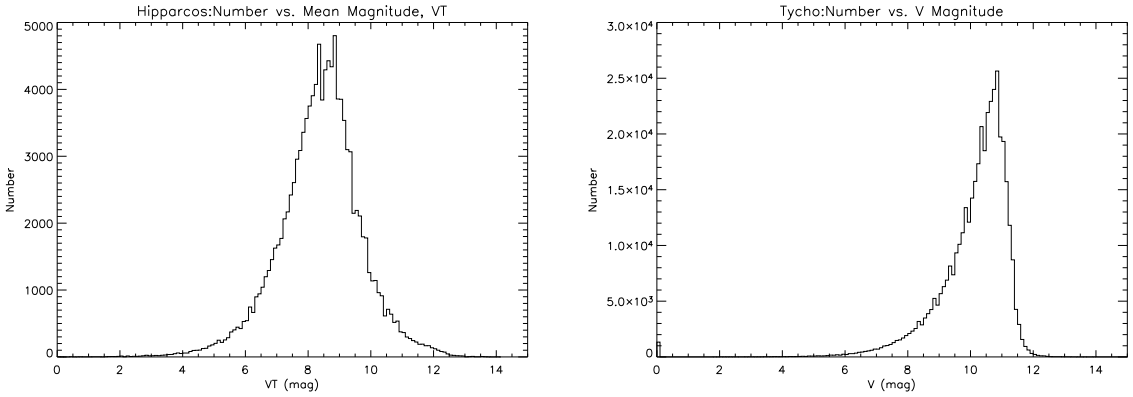

Fig. 12.— V magnitude histogram. Left:Hipparcos. Right:Tycho.

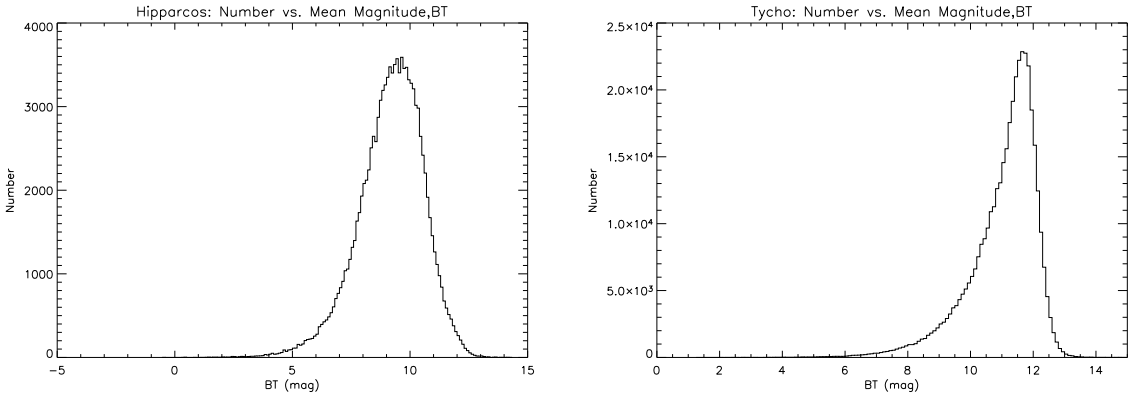

Fig. 13.— B magnitude histogram. Left:Hipparcos. Right: Tycho.

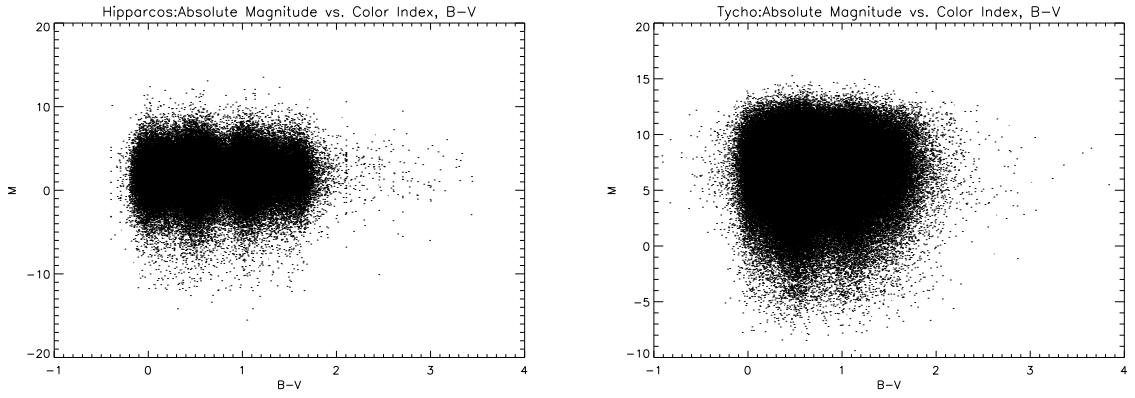

Fig. 14.— The HR diagram. Left:Hipparcos. Right: Tycho.

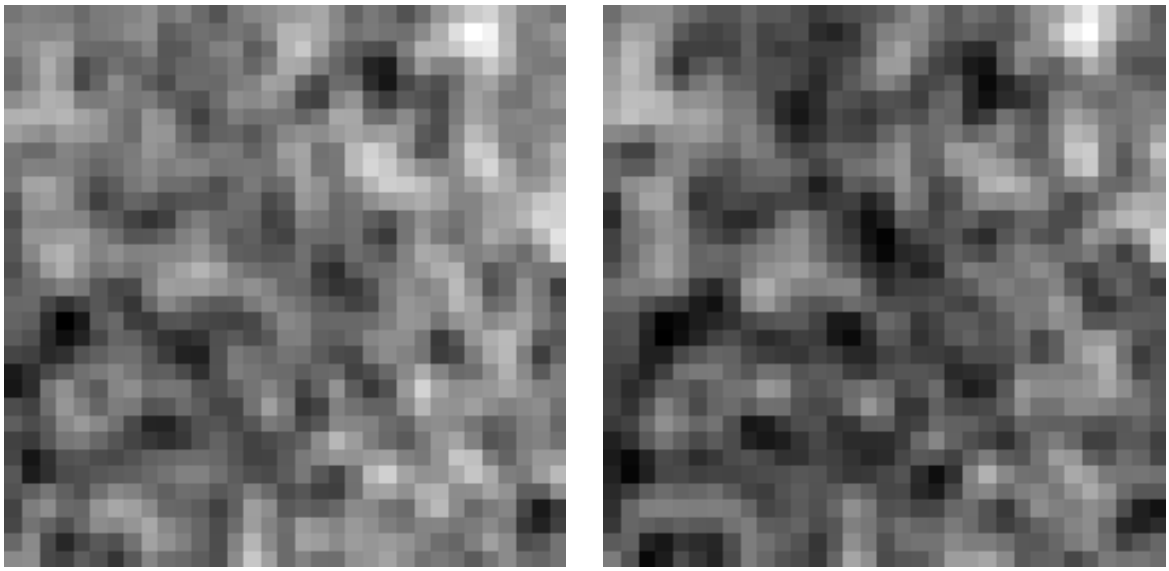

Fig. 15.— Left:All Hipparcos images for distance less than 10pc. 623 images used in stack. Image RMS is 5.65E-06. Right:All Hipparcos images for distance less than 25pc. Image RMS is 4.99E-06. Total number of stacked images 940.

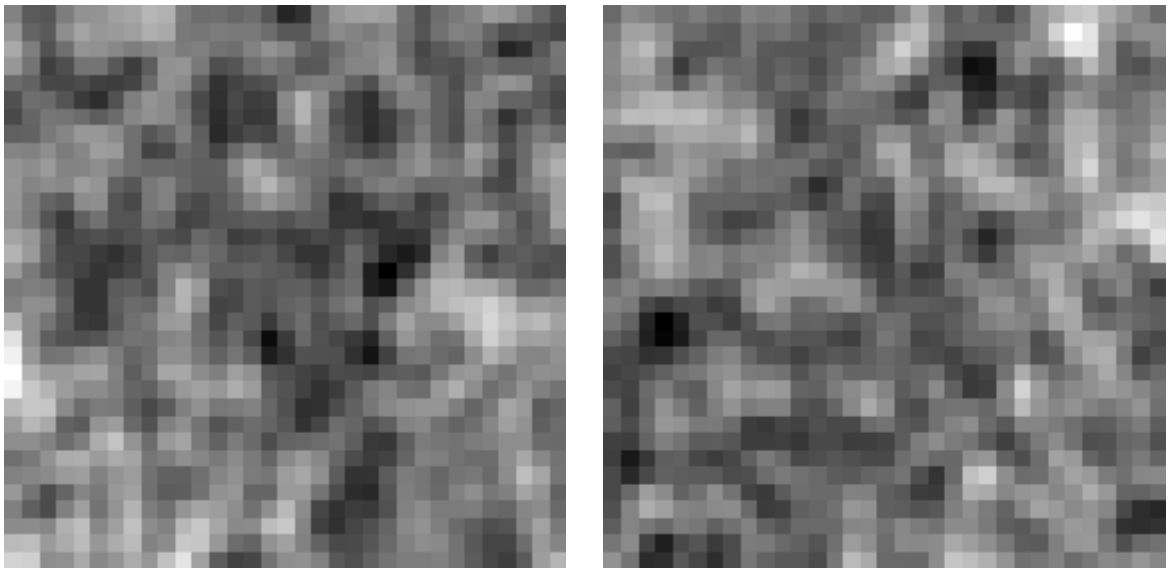

Fig. 16.— Left:Hipparcos M stars with a distance greater than 20pc. Image RMS is 1.14E-06. Total number of stacked sources is 18217. Right: Hipparcos M stars with a distance less than 20pc. Image RMS is 5.55E-06. Total number of stacked images is 736.

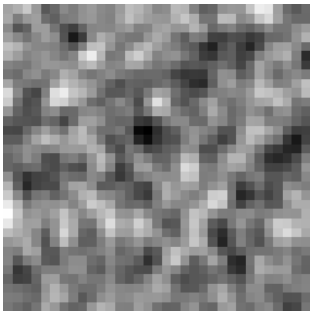

Fig. 17.— F stars with with B-V less than 0.3. Image RMS is 2.83E-06. Total number of stacked images is 2519.

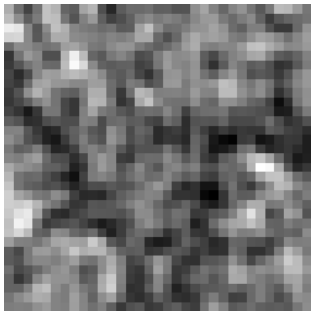

Fig. 18.— F stars with B-V between 0.3 and 0.58 and distance less than 450pc.Image RMS is 1.99E-06. Total number of stacked images is 5655.

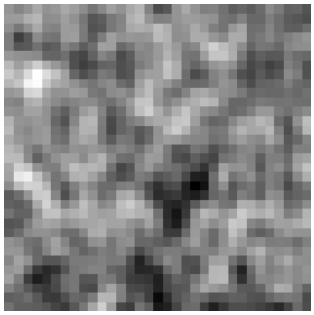

Fig. 19.— F stars with B-V between 0.3 and 0.58 and distance greater than 450pc. Image RMS is 5.25E-06. Total number of stacked images is 920.

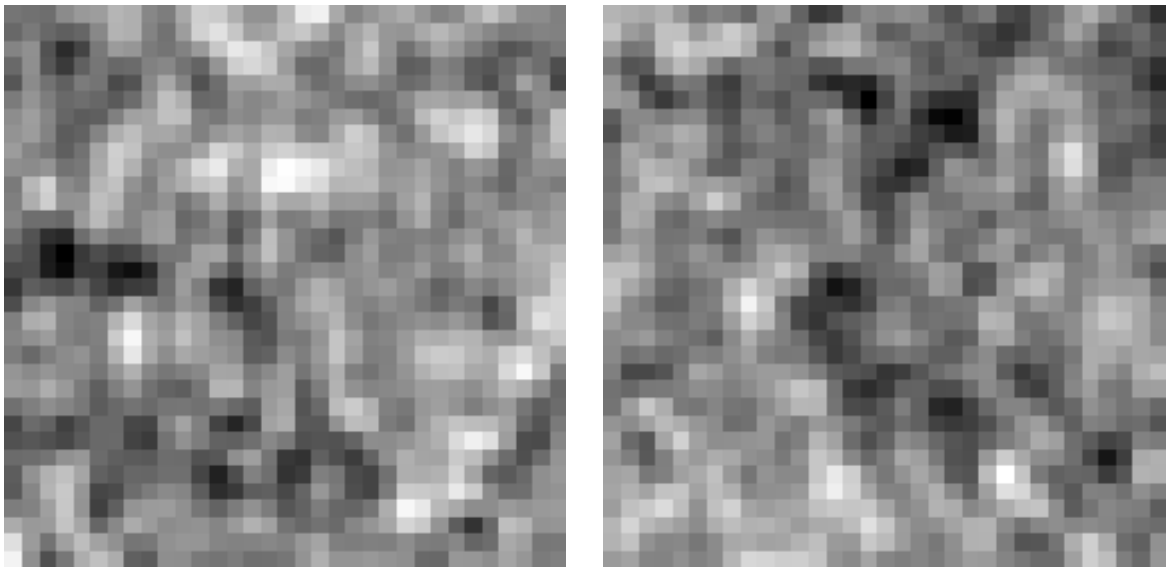

Fig. 20.— Left:Hipparcos G stars with B-V between 0.58 and 0.8 and a distance greater than 200pc. Image RMS is 4.32E-06. Total number of stacked images is 1046. Right: Hipparcos G stars with B-V between 0.58 and 0.8 and a distance less than 200pc. Image RMS is 3.99E-06. Total number of stacked images is 1363.

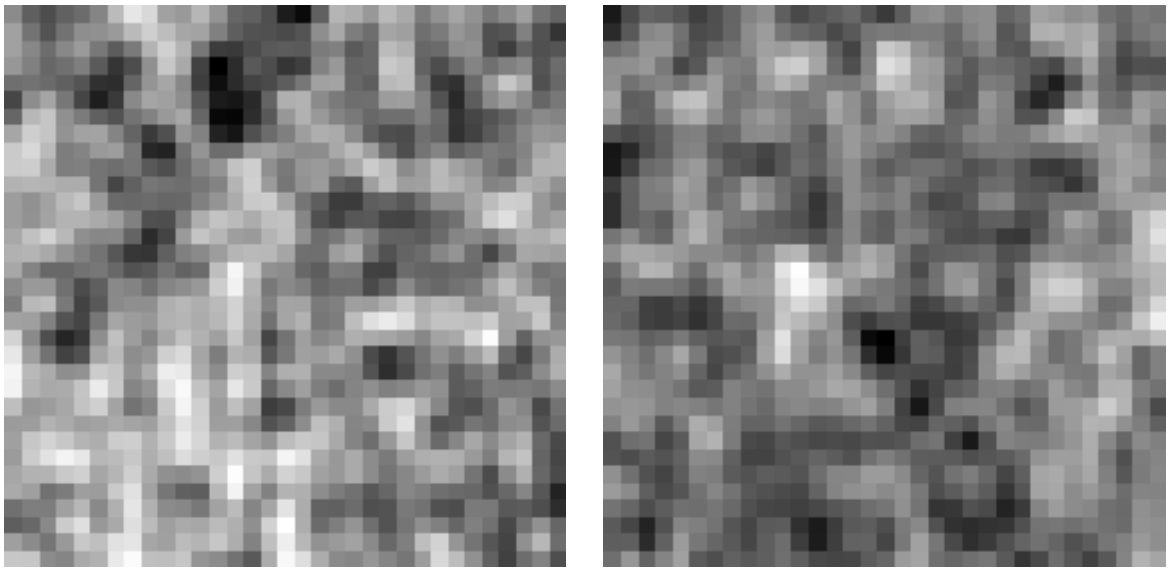

Fig. 21.— Left:Hipparcos K stars with B-V between 0.8 and 1.4 and a distance greater than 100pc. Image RMS is 3.45E-09. Total number of stacked images is 5485. Right: HipparcosG stars with B-V between 0.8 and 1.4 and a distance less than 100pc.Image RMS is 3.23E-06. Total number of stacked images is 1848.

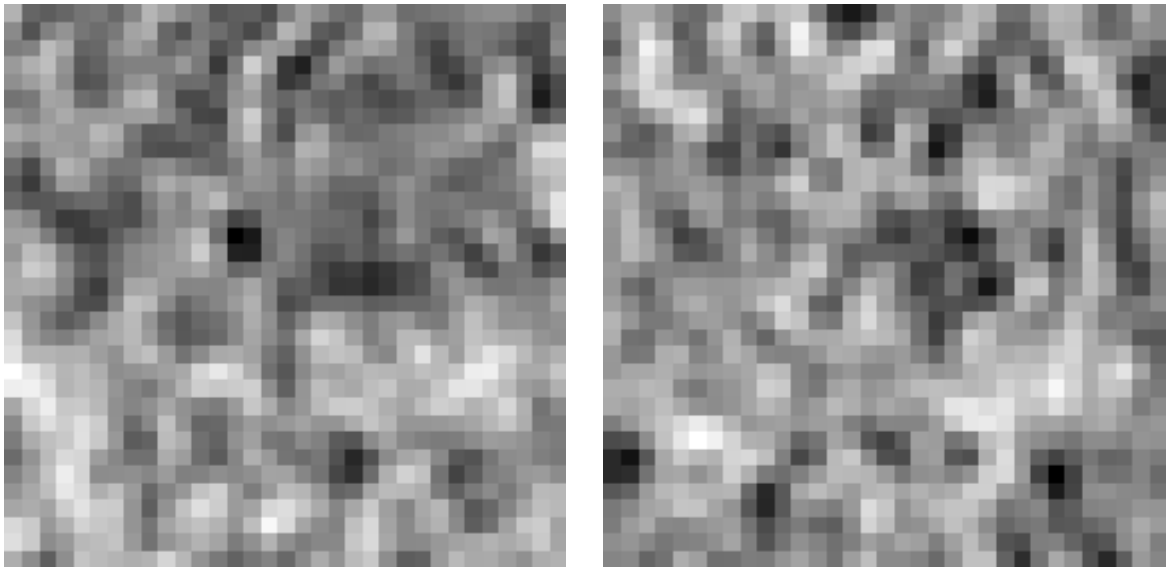

Fig. 22.— Historical status of the CCDM identifier. Left: No distance criteria. Image RMS is 2.53E-06. Total number of stacked images is 2851. Right: Distance less than 50pc. Image RMS is 8.50E-06. Total number of stacked images is 279.

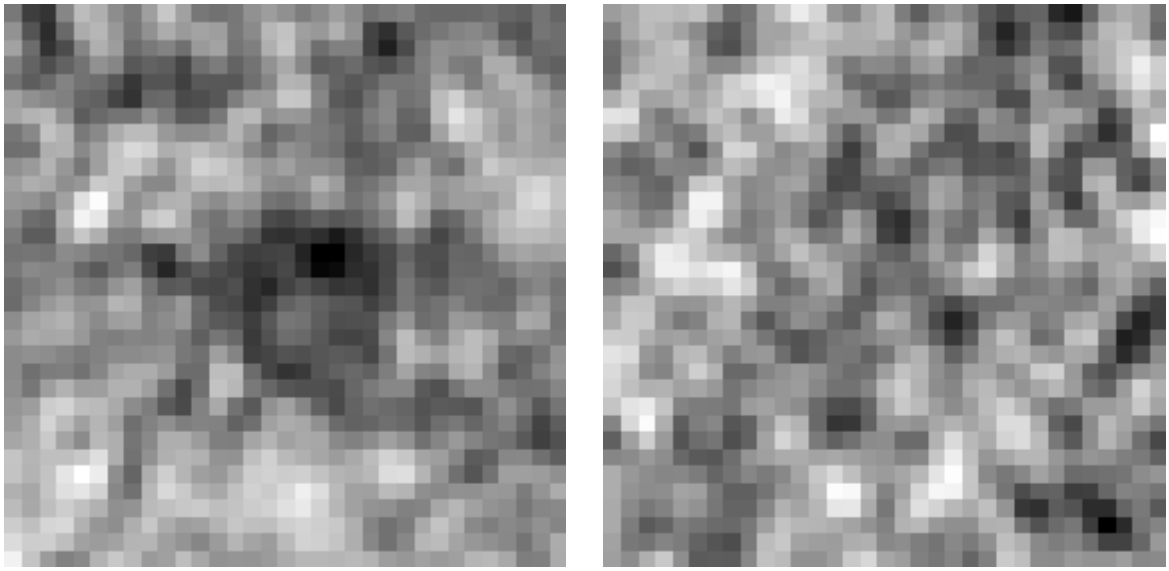

Fig. 23.— Selection Criteria for Tycho. Left: Kdwarfs. Image RMS is 1.09-06. Total number of stacked images is 26,279. Right: M stars. Image RMS is -1.9490E-06. Total number of stacked images is 6,065.

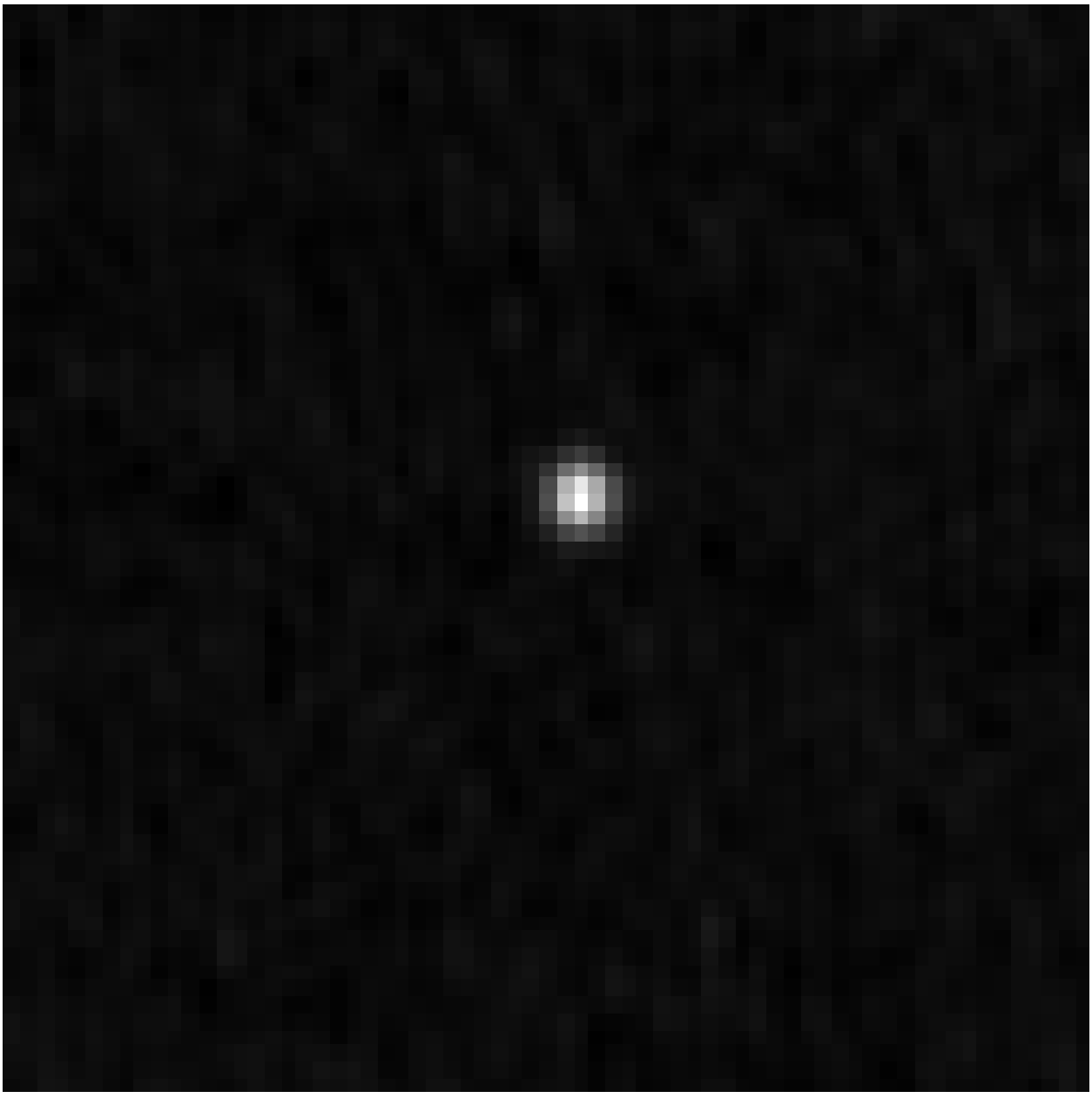

Fig. 24.— typical detected source.